ACTA IMEKO
ISSN: 2221-870X
June 2025, Volume 14, Number 2, 1 - 6

Observation of the evolution of the 25th solar cycle by measuring the ionospheric delay using the GPS P3 method in southeastern Brazil

Fábio K. Yamada[1], Luiz V. G. Tarelho[2], Mauro V. Lima[2]

[1] *Industrial Fostering and Coordination Institute – IFI, São José dos Campos, SP, Brazil*
[2] *National Institute of Metrology, Quality, and Technology – INMETRO, Duque de Caxias, RJ, Brazil*

ABSTRACT
Ionospheric refraction generates time delay and signal fading in the electromagnetic signals, which can cause errors in the receiver. These errors can range from a few meters in location to total signal unavailability, depending on the ionisation level of the ionosphere plasma. The parameter to evaluate the behaviour of the ionosphere is the Total Electron Content (TEC). This article will present the relationship between the evolution of the number of sunspots of the 25th solar cycle and the Vertical TEC (VTEC) measurement made by a geodetic receiver in the city of Xerém (Brazil). We applied the GPS P3 method of time and frequency transfer to the observables of the receiver. Periods related to the year's seasons (summer and winter) were analysed since the beginning of the 25th solar cycle in 2019. The VTEC analysis characterises the behaviour of the ionosphere caused by the daily, annual, summer, and winter variations in the incidence of solar radiation in southeastern Brazil. Therefore, the analysis can correlate the ionospheric fluctuation with the number of monthly sunspots, referring to the evolution of the 25th solar cycle. The findings of this study are expected to contribute to further developments of a deeper understanding of the ionosphere's dynamics and further advancements in GNSS-related services.

Section: RESEARCH PAPER

Keywords: GPS P3 method; ionosphere; ionospheric refraction; total electron content; TEC

Citation: F. K. Yamada, L. V. G. Tarelho, M. V. Lima, Observation of the evolution of the 25th solar cycle by measuring the ionospheric delay using the GPS P3 method in southeastern Brazil, Acta IMEKO, vol. 14 (2025) no. 2, pp. 1-6. DOI: 10.21014/actaimeko.v14i2.1969

Section Editor: Carlos Hall, PósMQI/PUC-Rio, Rio de Janeiro, Brazil

Received November 4, 2024; **In final form** June 17, 2025; **Published** June 2025

Corresponding author: Fábio K. Yamada, e-mail: yamadafky@fab.mil.br

1. THE IONOSPHERE PROBLEM IN GLOBAL NAVIGATION SATELLITE SYSTEMS (GNSS)

Ionospheric refraction is one of the most significant sources of error for GPS positioning and navigation [1]. It causes an increase in the path taken by the electromagnetic signal between the satellite and the terrestrial receiver. This error depends on the values of the signal frequency and the Total Electron Content (TEC) presented in the ionosphere plasma. The TEC is the main parameter to evaluate the behaviour of the ionosphere. Depending on its ionisation level, the measurement error can vary from a few meters in location to the loss of the signal link. The ionisation level of the ionosphere plasma is directly related to the geomagnetic field and solar radiation. This paper presents that it is possible to correlate the behaviour of TEC, measured with GPS P3 method, to the number of sunspots of the 25th solar cycle. For this purpose, Section 2 presents the method GPS P3 used for the realisation of Universal Time Coordinated (UTC), while Section 3, reports considerations of temporal and spatial variations of Brazil's southwestern area and the mathematical modelling. Results and analysis are contained in Section 4, while Section 5 reports the conclusions.

2. THE METHOD GPS P3 OF TIME AND FREQUENCY TRANSFER AND THE MEASUREMENT OF IONOSPHERIC DELAY

To acquire compliance with services demanding precise synchronisation, such as energy distribution, telecommunications systems, and financial processes in stock exchanges, local time scales designated as UTC(k) are utilised. These scales play a crucial role in the preparation of UTC, a globally accepted time standard overseen by the *Bureau International des Poids et Mesures* (BIPM).

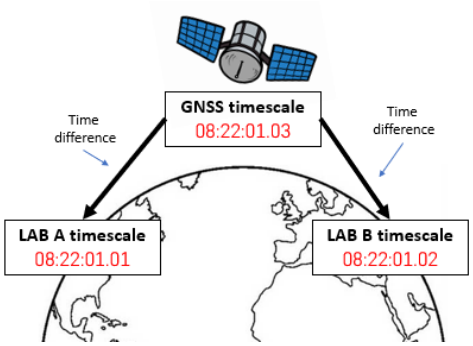

Figure 1. Concept of time and frequency transfer (from the author).

Daily, local UTC(k) establishes transmission of standardised information to the BIPM. Subsequently, the BIPM processes and calculates the *Echelle Atomique Libre* (EAL) or Free Atomic Scale, which is aligned with the definition of the second within the International System of Units (SI). The EAL is steered by a comparison with highly accurate primary and secondary frequency standards. This process ultimately yields International Atomic Time (TAI) [2].

The final step involves a comparison between UTC and Universal Time (UT1), which is based on the Earth's rotation. If a discrepancy larger than 0.9 seconds is detected, an additional second, known as a "leap second", is introduced to maintain synchronisation with the non-uniform time derived from the Earth's rotation [2].

At the end of the UTC process, the BIPM releases a document called Circular T which presents the time difference of each local time scale with UTC, allowing the participating laboratories to apply corrections so that their time scales remain close to UTC [3]. In Brazil, the National Institute of Metrology, Quality, and Technology (INMETRO) contributes with the physical realisation UTC(INXE) to the calculation of the UTC.

GNSS satellites are used in the UTC calculation process. They have embedded atomic clocks that make it possible to compare the time scales and the realisation of the UTC. The local time scales, UTC(k), are compared to GNSS system time (GNSS time) using geodetic receivers connected to 1 PPS (pulse per second) and 10 MHz outputs of the time scale. Considering the difference related to a common GNSS time, two or more laboratories can compare their time scales. This setup allows the generation of the CGGTTS (CCTF Group on GNSS Time Transfer Standards) file, whose main function is to standardise the comparison of time scales. The concept of time and frequency transfer is shown in Figure 1.

The **CGGTTS** file has been widely used as a standard format for time and frequency analysis using GNSS receivers. It covers the satellite constellations such as GPS, Glonass, Galileo, and Beidou. The **CGGTTS** files predict eliminating ionosphere delay at the first-order effects by combining the GPS signals' P1 and P2 codes [4]. This technique is known as P3 code or ionosphere-free code and allows to detect and correct up to 90% of the ionospheric effect [5]. Figure 2 shows the table within a CGGTTS file.

Measurements are sampled every 30 seconds and are consolidated into blocks of 16 minutes. The average number of satellites observed per measurement interval varies according to the line of sight (LOS), the system configuration, and installation. It is common 5 to 10 satellites per block being measured for GPS. The information used for the analysis of ionospheric delay and calculation of the TEC is shown in Figure 2, highlighted in the green columns, and it is described as:

- **MJD**: **M**odified **J**ulian **D**ay;
- **STTIME**: **ST**art **TIME** of the measurement interval in hours, minutes, and seconds; and
- **MSIO**: **M**ea**S**ured **IO**nospheric Delay of L1 signal (1.575,42 MHz) of GPS.

3. THE TOTAL ELECTRON CONTENT (TEC) IN THE SOUTHEASTERN REGION OF BRAZIL

The ionosphere is located between 50 to 1000 km altitude, and its composition is made up of electrically charged particles called ions. It has a density capable of altering the propagation of electromagnetic waves [6]. The Total Electron Content (TEC) represents the number of electrons in the electromagnetic signal's path between the satellite and the terrestrial receiver [7]. TEC is measured in a unit of 10^{16} electrons per m^2, equivalent to 1 TECU (TEC Unit).

The ionisation level of the plasma mainly depends on the solar radiation and geomagnetic conditions of the region, namely, the higher the intensity of solar radiation and the lower the intensity of the magnetic field of the area, the greater the error caused by ionospheric refraction in the electromagnetic signal. Brazil's southeastern region has a lower magnetic field intensity due to a magnetic anomaly known as South Atlantic Magnetic Anomaly (SAMA). The summer period (December to March), where the intensity of solar radiation is higher than the other periods of the year, associated with SAMA presents a scenario that contributes to a significant error caused by ionospheric refraction.

3.1. South Atlantic Magnetic Anomaly (SAMA)

The UTC(INXE) is in the district of Xerém, municipality of Duque de Caxias (RJ) (22° S; 45° W), which is considered an ionospheric geographical region of low latitude. However, this region has a high level of electron density [6], similar to an equatorial latitude, due to an anomaly. The phenomena related to the Equatorial Ionisation Anomaly (especially in periods of more significant solar activity) can occur in this region, which presents a peak in electron density in the afternoon and a second peak at dusk [8].

The Earth's magnetic field acts as a shield against electrically charged particles coming from space. Depending on the intensity of these particles, a change in the density of terrestrial electrons occurs. This can affect the ionosphere, causing, consequently, impacts on the signal links between satellites and terrestrial

SAT	CL	MJD	STTIME	TRKL	ELV	AZTH	REFSV	SRSV	REFSYS	SRSYS	DSG	IOE	MDTR	SMDT	MDIO	SMDI	MSIO	SMSI	ISG	FR	HC	FRC	CK
			hhmmss	s	.1dg	.1dg	.1ns	.1ps/s	.1ns	.1ps/s	.1ns		.1ns	.1ps/s	.1ns	.1ps/s	.1ns	.1ps/s	.1ns					
G01	FF	59902	001400	780	697	2443	-1942510	49	555293	-7	25	78	81	-2	352	43	352	43	26	0	0	L3P	4C
G03	FF	59902	001400	780	402	2060	4289188	1	555291	-16	35	68	117	-11	378	-44	378	-44	27	0	0	L3P	7D
G04	FF	59902	001400	780	416	2701	1395260	16	555292	83	41	86	114	-7	742	-195	742	-195	38	0	0	L3P	9A
G21	FF	59902	001400	780	675	3431	-1002308	8	555274	0	39	27	82	5	411	61	411	61	38	0	0	L3P	07
G22	FF	59902	001400	780	234	1402	-3118504	-168	555327	-90	86	26	190	44	255	72	255	72	76	0	0	L3P	92
G31	FF	59902	001400	780	413	1248	2561485	-11	555304	-24	32	88	115	11	239	18	239	18	26	0	0	L3P	65
G01	FF	59902	003000	780	724	2692	-1942484	68	555266	13	29	78	80	0	438	79	438	79	25	0	0	L3P	61

Figure 2. Table of a CGGTTS file (from the author).

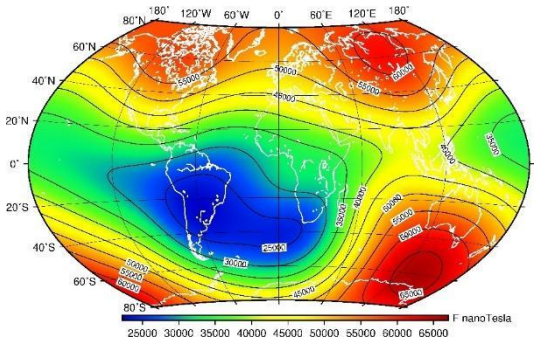

Figure 3. Total magnetic field strength [10].

receivers [9]. According to the International Geomagnetic Reference Field (IGRF), an example of the total strength of the magnetic field is shown in Figure 3.

The IGRF is updated every five years and describes the field from 1900 to 2025 [10]. Figure 3 shows the SAMA localised in Latin America, especially in Brazil. This region has a lower magnetic field intensity than the rest of the planet. In SAMA, the particles spiral in the magnetic field lines at around 100 km altitude, while for other regions, this process occurs at about 600 km altitude [11].

3.2. Solar activities and the 25th solar cycle

The Sun, responsible for the source of radiation, presents cycles of short and long-duration activities. Long-term cycles average 11 years and emit more radiation in specific periods. At the peaks of solar cycles, events such as explosions and ejections of coronal masses become more frequent. These events release amounts of charged particles that reach the Earth and cause disturbances in the geomagnetic field. Typically, solar flares are associated with the most active regions of the solar surface, identified as **sunspots**.

Thus, one way to monitor the solar cycle is through the number of sunspots. At the beginning of the cycle, the number of sunspots is minimal; at the apex, the number of sunspots is maximum [12]. The 25th Solar Cycle, which began in mid-2019, is currently in progress. Figure 4 presents a history of the last three solar cycles containing the curves of the amounts of sunspots (black colour) and the prediction of the current and 25th solar cycle. The current cycle shows a behaviour above the expected since the number of sunspots measured is above the predicted values and range.

Ionospheric refraction depends on the frequency of the signal that travels through it as well, according to

$$v = \frac{40.3}{c\, f^2} \cdot TEC\,, \tag{1}$$

where v is the ionospheric delay in s, c the speed of light in (m/s), 40.3 a constant [m³/(s² electrons)], f the wave frequency in (1/s) and TEC the Total Electron Content in (electrons/m²).

Equation (1) shows that the delay is inversely proportional to the square of the frequency. Even for a GPS using a relatively high frequency of the L1 signal at the value of 1.575 GHz, it may suffer a significant ionosphere delay.

3.3. VTEC calculation using GPS P3 method

Considering that the elevation of the satellites varies depending on their location, the distances between the receiver antenna and the satellites also vary. Consequently, the TEC values will vary proportionally. In such sense, the single-layer ionospheric model (SLM) [14] concept is generally applied in ionosphere modelling research derived from GNSS. SLM considers that all free electrons are concentrated in a layer of infinitesimal thickness. The altitude of this layer varies according to the model adopted by each tool, with values between 350 km and 450 km being common.

The layer's altitude defines the location of the ionospheric point or IPP (Ionospheric Pierce Point), which is the point of intersection in the line of sight between the satellite and the receiver, which passes through this layer. The projection of the IPP on the Earth's surface is called the sub-ionospheric point [15]. Thus, using the SLM concept, which considers that all electrons are concentrated in the layer, and determining the coordinates of the ionospheric point, it is possible to generate a grid with the TEC values distributed over the layer. One way to apply the SLM is by using the trigonometric function, described according to [14]:

$$F_{\mathrm{I}}(z) = \frac{E}{E_v} = \frac{1}{\cos z'}\,, \tag{2}$$

where E and E_v are the TEC values contained in the line of sight (between the satellite and the receiver antenna) and in the

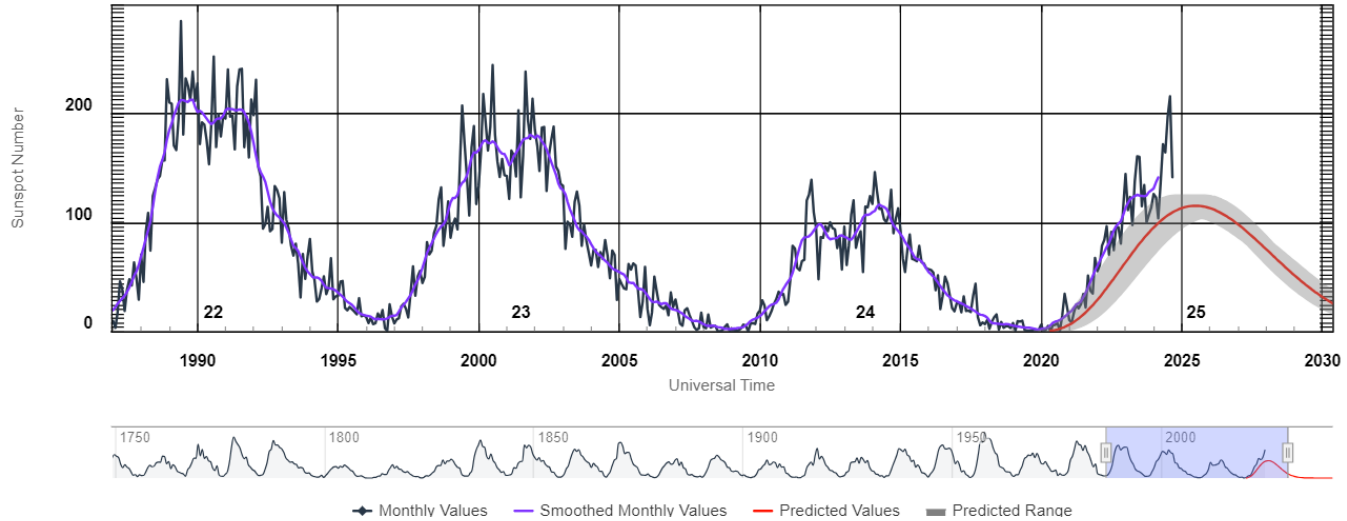

Figure 4. Solar cycle sunspot number progression [13].

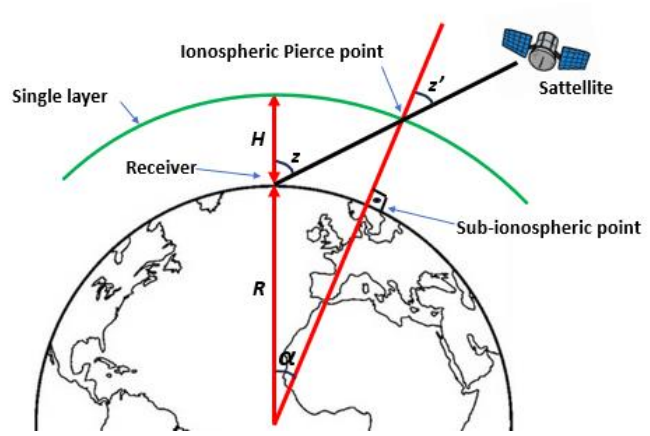

Figure 5. Single Layer Model (from the author).

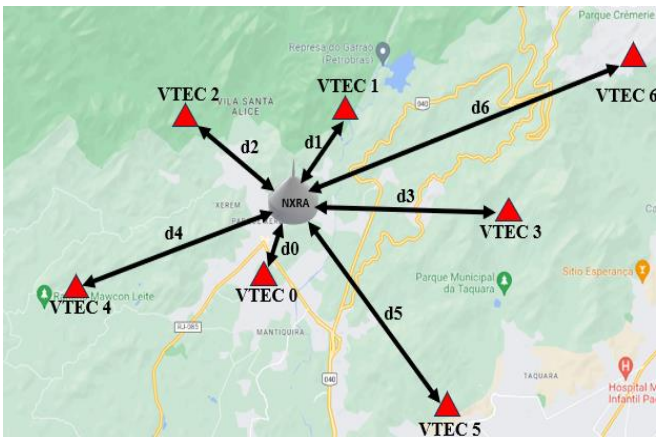

Figure 6. Example of a group of 16-minute VTEC measurements (from the author).

vertical projection of the IPP, respectively. To calculate $\cos z'$ it is necessary to calculate $\sin z'$ first, according to

$$\sin(z) = \frac{R}{R+H} \cdot \sin(z'), \tag{3}$$

where z and z' are the zenith angles at the terrestrial receiver antenna and at the IPP, R is the radius of the Earth and H is the height of the simple ionospheric layer of the Earth.

Figure 5 illustrates the SLM concept where IPP is the intersection in the line of sight between the receiver and the satellite, the sub-ionospheric point is the projection of the IPP, H is the altitude of the single layer and α, z, and z' are the angles.

The geographical latitude (ϕ_{ip}) and longitude (λ_{ip}) of the IPP, at a given altitude (h_{ip}), are obtained from the azimuth and elevation angles of the GNSS signal according to [16], [17]:

$$\phi_{\text{ip}} = \arcsin[\sin\phi_r \cos\psi + \cos\phi_r \sin\psi \cos Az] \tag{4}$$

$$\lambda_{\text{ip}} = \lambda_{\text{r}} + \arcsin\left[\frac{\sin(\psi)\sin(Az)}{\cos(\phi_{ip})}\right] \tag{5}$$

with

$$\psi = \frac{\pi}{2} - El - \arcsin\left[\frac{r_{\text{e}}}{(r_{\text{e}} + h_{\text{ip}})}\cos(El)\right], \tag{6}$$

where ϕ_{r} and λ_{r} are the latitude and longitude of the terrestrial receiver in radians, r_{e} is the radius of the Earth equal to 6371 km, Az and El are the azimuth and elevation angles of the GNSS signal in radians, and h_{ip} is the altitude of the IPP layer (usually 350 km or 450 km).

4. EXPERIMENTS, RESULTS, AND ANALYSIS

The concept of SLM were necessary to calculate the "vertical" ionospheric delay to obtain the respective VTEC, according to Equation 2. Then, using the elevation, azimuth, and altitude of each signal and the single layer equal 450 km, the location coordinates of the sub-ionospheric point are determined. Considering that the sub-ionospheric points are at the same altitude as the receiver antenna, the distances of each sub-ionospheric point about the receiver antenna are calculated. Thus, for each group of 16 min measurements, the average VTEC weighted by distances is calculated, that is, the closest VTEC having a more significant weight about the VTEC furthest from the receiver.

For example, Figure 6 presents seven measurements (d_0 to d_6) relative to an interval of 16 min. Each VTEC measurement (Δ) has a distance d_0 from the location of the NXRA receiver antenna, with d_0 being the smallest distance and d_6 being the largest distance.

First, the latitude and longitude of each IPP must be calculated to calculate distances. For these purposes, the geometric method presented in equations (4), (5), and (6) is applied using the elevation and azimuth of each measurement, available, respectively, in the ELV and AZTH columns of the CGGTTS file. With the coordinates determined, the distances are calculated, and finally, the average value of VTEC measurements is calculated for each 16-minute interval, weighted by distances, according to:

$$VTEC_{\text{Méd Pond}} = \frac{\sum_{i=0}^{n} E_i \left(\frac{d_0}{d_i}\right)}{\sum_{i=0}^{n} \frac{d_0}{d_i}} \tag{7}$$

with d_0 being the shortest distance, d_i being the distance to the IPP of satellite i, E_i being the VTEC corresponding to the IPP of satellite i and satisfying the condition $d_i < d_{i+1}$.

The total measurement uncertainty of the VTEC measured by the GPS P3 method for each 16-minute measurement group is calculated using Equation 8

$$\sigma_{\text{VTEC TOTAL}} = \sqrt{\sigma^2_{\text{VTEC B}} + \sigma^2_{\text{VTEC A}}}, \tag{8}$$

where $\sigma_{\text{VTEC A}}$ is the measurement uncertainty of Type A and $\sigma_{\text{VTEC B}}$ is the measurement uncertainty of Type B.

Measurements were conducted over ten periods of the 25th solar cycle, with five occurring in the summer (January) and five in the winter (July), starting from 2020. The values of the MSIO column of the CGGTTS and equation (1) were used to calculate the TEC. The measurements were consolidated every hour, obtaining the mean and repeatability uncertainty, for an overall 24 daily measurements. Next, the hourly and repeatability uncertainty averages of each hour and month were calculated according to Figure 7.

It is possible to observe the behaviours related to the daily, annual, and seasonal variations regarding the intensity of solar radiation in the ionosphere. During the day, it is possible to verify

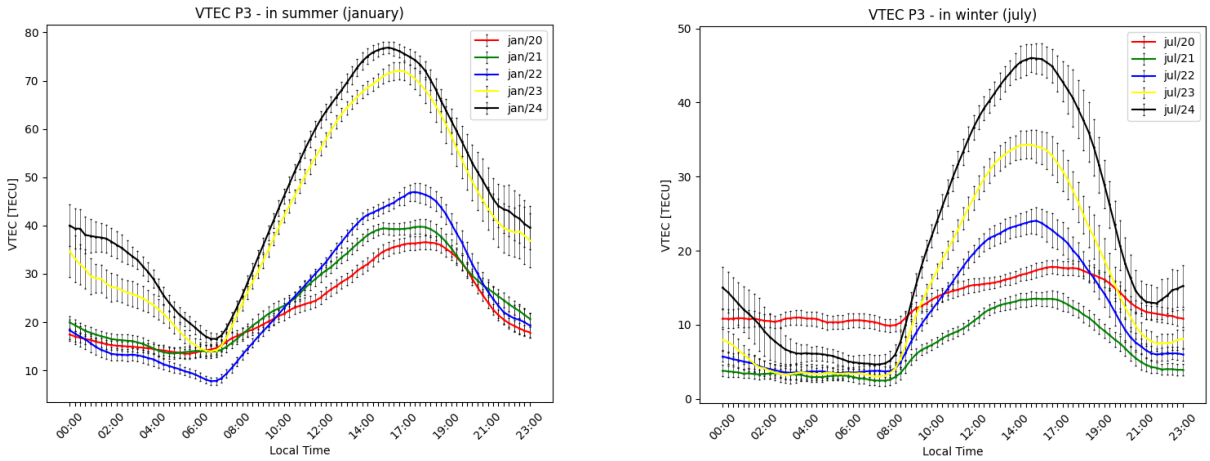

Figure 7. Average VTEC for the summer and winter months (from the author).

that the VTEC is higher between 12 h and 24 h (summer) and 12 h and 20 h (winter) due to the higher incidence of solar radiation. At other times of the day, the values are lower and more stable; in the summer months (except for January 2023 and January 2024), the values remain around 10 and 30 TECU, and in the winter months, they stay at approximately 5 to 15 TECU.

Regarding the behaviour of the seasons, it is observed that the amplitude of the values of the summer months is greater than that of the winter months for each year, respectively. An example at hand is the year 2022, where in January we have a maximum value of around 45 TECU, and in July, around 25 TECU. In 2023, January had an average maximum value of approximately 70 TECU; in July an average maximum of around 35 TECU. When evaluating only the months of each season, we have an annual increase in the amplitude between the summer months. In 2020, we have a maximum average value starting around 35 TECU, followed by 40 TECU (2021), 45 TECU (2022), 70 TECU (2023) and reaching 75 TECU (2024). Regarding the winter months, we started with the month of July 2020 with about 18 TECU, followed by a decrease to about 12 TECU (2021), the following year, an increase to about 25 TECU (2022), then another increase to about 33 TECU (2023) and ending in July 2024 with about 45 TECU.

Then, for each period, the correlation was made between the VTEC amplitude (VTEC max – VTEC min) values and the number of sunspots, obtaining the graphs presented in Figure 8.

It is possible to observe a correlation between the VTEC amplitude and the number of sunspots in the solar cycle. At the beginning of the cycle, the variation of both is slight; however, with the increase in the number of sunspots, the variation of the VTEC also sharper increase.

5. CONCLUSION

The experiment presented in this article highlighted that it is possible to correlate daily, annual and seasonal variations of the Vertical Total Electronic Content (VTEC) with the solar sunspots.

It was also possible to correlate the monthly variations of the VTEC with the number of sunspots of the 25th solar cycle. It should be noted that this cycle presents an average of sunspots higher than expected, and its peak is expected to occur in the middle of the year 2025. In this sense, the ionosphere will affect even more the GNSS signals in the near future.

AUTHORS' CONTRIBUTION

Writing – original draft – Fábio K. Yamada
Methodology – Fábio K. Yamada and Luiz V. G. Tarelho
Conceptualization – Luiz V. G. Tarelho
Data curation – Fábio K. Yamada, Luiz V. G. Tarelho and Mauro V. Lima
Writing – review & editing – Luiz V. G. Tarelho and Mauro V. Lima

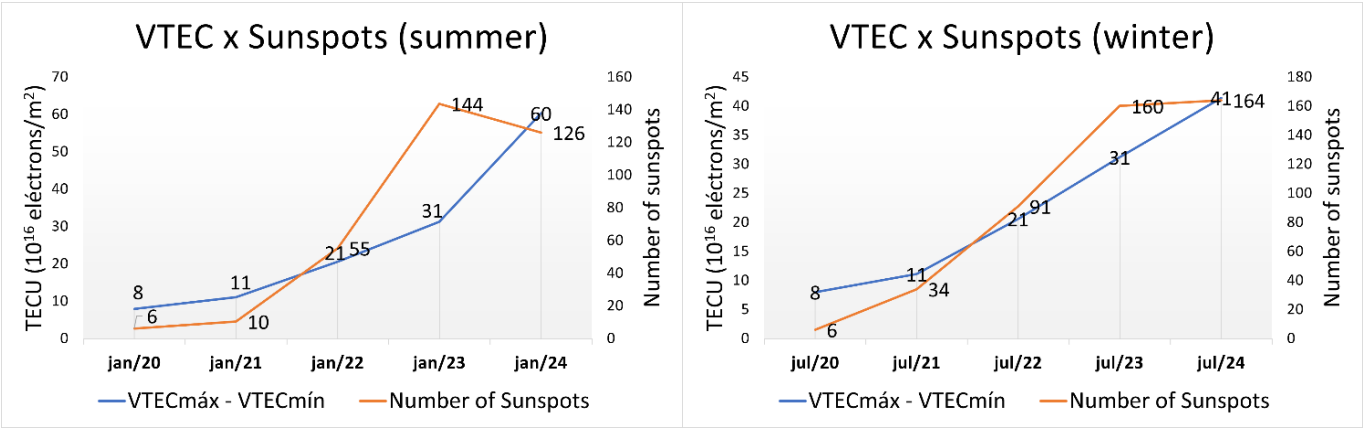

Figure 8. Correlation between the number of sunspots and VTEC (from the author).

ACKNOWLEDGEMENT

We would like to thank the technical groups of the Aerospace Metrological Reliability Division (CMA) of the Industrial Fostering and Coordination Institute (IFI) and the Metrology in Information Technology and Telecommunications Division (DMTIC) of the National Institute of Metrology, Quality, and Technology (INMETRO) for supporting this research.

REFERENCES

[1] P. C. L. Segantine, GPS - Sistema de Posicionamento Global vol 1 (São Carlos), 2005. [in Portuguese]

[2] G. Panfilo, F. Arias, The Coordinated Universal Time (UTC) Metrologia 56, 2019, 042001. DOI: https://doi.org/10.1088/1681-7575/ab1e68

[3] BIPM, 2023 Circular T, BIPM website. Online [Accessed 23 June 2025] https://www.bipm.org/en/time-ftp/circular-t

[4] P. Defraigne, G. Petit, CGGTTS-Version 2E: an extended standard for GNSS Time Transfer, Metrologia, 52, 2015, G1–G1. DOI: http://dx.doi.org/10.1088/0026-1394/52/6/G1

[5] ITU, ITU-T Technical Report 2020 GSTR-GNSS Considerations on the use of GNSS as a primary time reference in telecommunications. Online [Accessed 23 June 2025] https://www.itu.int/dms_pub/itu-t/opb/tut/t-tut-home-2020-pdf-e.pdf

[6] M. T. Matsuoka, P. de O. Camargo, I. S, Batista, Impacto de explosões solares no comportamento da ionosfera e no posicionamento com GPS na região brasileira: Estudo de caso para o dia 28 de outubro de 2003 Boletim de Ciências Geodésicas 12, 2006, pp. 315–34. [in Portuguese]

[7] V. A. dos Santos, Uso de dados de redes GNSS ativas para a geração de mapas regionais ionosféricos (Presidente Prudente), 2020. [in Portuguese]

[8] S. F. de Souza, M. T. Matsuoka, Efeitos da ionosfera nas observáveis GPS e no posicionamento por ponto na região brasileira: Revisão e síntese das investigações realizadas. Série em Geomática 2, 2008, pp. 29–38. [in Portuguese]

[9] E. Frigo, G. Hartmann, Variações de intensidade do campo geomagnético em Santa Maria (Brasil) para os últimos 3 mil anos Ciência e Natura 40 7, 2018. [in Portuguese]

[10] British Geological Survey, 2023 International Geomagnetic Reference Field (IGRF) website. Online [Accessed 23 June 2025] https://geomag.bgs.ac.uk/research/modelling/IGRF.html

[11] T. Jaskulski, H. C. Aveiro, L. P. Moor, C. M. Denardini, P. Muralikrishna, N. J. Schuch, Estudo do plasma ionosférico da anomalia magnética do Atlântico Sul (AMAS) utilizando riômetros, 2006. [in Portuguese]

[12] NASA, Space Place 2023 Whats is the Solar Cycle? website. Online [Accessed 23 June 2025] https://spaceplace.nasa.gov/solar-cycles/en/

[13] NOAA, Space Weather Prediction Center, Solar Cycle Progression, 2023, website. Online [Accessed 23 June 2025] https://www.swpc.noaa.gov/products/solar-cycle-progression

[14] R. Dach, U. Hugentobler, P. Fridez, M. Meindl, Bernese GPS Software Version 5.0, 2007, pp. 258–60.

[15] X. Yang, J. Li, S. Zhang, Ionospheric correction for spaceborne single-frequency GPS based on single layer model, J Earth Syst Sci 123, pp. 767–778. DOI: https://doi.org/10.1007/s12040-014-0442-z

[16] M. T. Matsuoka, P. de O. Camargo, Correção Ionosférica utilizando os mapas globais do TEC do IGS: Avaliação no posicionamento por ponto na região brasileira Boletim Ciências Geodésicas 13, 2007, pp. 253–70. [in Portuguese]

[17] F. dos S. Prol, P. de O. Camargo, M. T. D. A. H. Muella, Estudo comparativo de métodos para calcular pontos ionosféricos e descrever o trajeto do sinal GNSS Boletim de Ciencias Geodesicas 23, 2017, pp. 669–83. [in Portuguese]